

Contents lists available at [SciVerse ScienceDirect](http://www.sciencedirect.com)

Tunnelling and Underground Space Technology

journal homepage: www.elsevier.com/locate/tust

Groutability of granular soils using sodium pyrophosphate modified bentonite suspensions

Jisuk Yoon^a, Chadi El Mohtar^{b,*}^a *Fugro Consultants Inc., 6100 Hillcroft, Houston, TX 77081, United States*^b *Department of Civil, Architectural and Environmental Engineering, The University of Texas at Austin, Austin, TX 78712-0280, United States*

ARTICLE INFO

Article history:

Received 24 May 2012

Received in revised form 26 October 2012

Accepted 1 April 2013

Keywords:

Permeation grouting

Groutability

Bentonite suspension

Sodium pyrophosphate

Rheology

ABSTRACT

Groutability of granular soils using sodium pyrophosphate (SPP) modified bentonite suspensions was studied to investigate its applicability in permeation grouting. While the relative grain size of the soil and the grout has been widely used to evaluate the groutability of granular soils with particulate grouts, such criteria do not account for the effect of chemical modifications of grouts such as the changes in their rheological properties. The modification of grouts may improve the depth of its penetration, and thus changing the groutability of the granular soils. For such cases, the rheological properties of grouts become crucial to evaluate groutability of soils. In this study, the rheological properties of bentonite suspensions were measured at various bentonite fractions (5%, 7.5%, 10%, and 12% by total mass of suspension) modified with 0%, 1%, 2%, 3%, and 4% SPP (by mass of dry bentonite), respectively. The small amounts of SPP effectively improved the mobility of the concentrated bentonite suspensions allowing the evaluation of change in groutability at different rheological properties but same concentrations. The modified bentonite suspensions were injected into the saturated sand columns prepared at various experimental conditions (effective particle size, relative density, and fines content) under two different constant pressures (35 and 140 kPa). The results showed that the injected pore volumes increased with an increase of the apparent viscosity at equilibrium (high shear rates). A new groutability criterion for granular soils is proposed based on the rheological properties of the suspensions, relative density of the sand, relative grain size of the sand and bentonite, and injection pressure. The proposed groutability criterion provides a more accurate prediction of groutability in granular soils when using modified bentonite suspensions.

© 2013 Elsevier Ltd. All rights reserved.

1. Introduction

Permeation grouting is a conventional technique to reduce hydraulic conductivity and strengthen ground by permeating low viscosity fluids into soils without disturbing original soil structure. While cement-based grouts have been widely used in practice, bentonite can be an alternative grout with environmental friendliness and long term safety (Moore et al., 1982; Chegbeleh et al., 2009). Recently, the possible application of bentonite grout has been studied for controlling hydraulic conductivity of clean sands (Hwang et al., 2011) and improving soil performance under static and seismic loading conditions (Haldavnekar et al., 2003; El Mohtar et al., 2008; Rugg et al., 2011).

However, application of the groutability criteria developed for cement-based grouts to bentonite suspensions becomes challenging because bentonite-based and cement-based grouts differ in their rheological properties as well as their particle size and shape,

even though they are both particulate suspensions. Moreover, most of the existing criteria are based on the groutability number (N), which considers only the penetration of a grout through a soil with the relative grain size of the soils and cements (Bell, 1993; Burwell, 1958; Incecik and Ceran, 1995), and do not include any information on the grout propagation through a soil. In addition, these criteria do not reflect the changes in rheological parameters of the different types of materials utilized, particularly when using super plasticizers in cement grouts. Markou and Atmatzidis (2002) reported that the use of the relative grain size for fly ash grouts produced relatively optimistic prediction of the groutability but with large variations in the experimental results. An advanced criterion suggested by Akbulut and Saglamer (2002) considered different parameters, of both soils and grouts, affecting groutability of granular soils such as fines content (FC), injection pressure (P), relative density (D_r), and water/cement ratios (w/c). However, this advanced criterion did not include the effect of super-plasticizers and therefore, producing the same groutability for a given granular soil and water/cement ratio regardless of the presence of super-plasticizers. Santagata and Santagata (2003) and Smoak and Mitch-

* Corresponding author. Tel.: +1 512 471 3695; fax: +1 512 471 6548.

E-mail address: ElMohtar@mail.utexas.edu (C. El Mohtar).

Nomenclature

C	empirical constant for the global model	IPv	the injected pore volume of grouts
Cc	coefficient of curvature	N	groutability of soil
Cu	coefficient of uniformity	N_c	Burwell's (1958) second groutability ($D_{10,sand} / d_{95,bentonite}$)
COV	coefficient of variation	N^*	new groutability for the modified bentonite suspensions
D	the diameter of filter materials (mm)	n	empirical constant for the global model
D_{10}	effective grain size of soil (mm)	P	injection pressure (kPa)
D_{15}	the diameter through which 15% of total soil mass is passing (mm)	SP	poorly graded sand
D_{30}	the diameter through which 30% of total soil mass is passing (mm)	SPP	sodium pyrophosphate
D_{60}	the diameter through which 60% of total soil mass is passing (mm)	USCS	unified soil classification system
d_{85}	the diameter through which 85% of total grout mass is passing (mm)	τ	shear stress (Pa)
d_{95}	the diameter through which 95% of total grout mass is passing (mm)	γ	shear strain (%)
Dr	relative density (%)	$\dot{\gamma}$	shear rate (1/s)
$Dr_{skeletal}$	skeletal relative density (%)	μ_{pL}	plastic viscosity (mPa s) viscosity that represents pure viscous behavior in Bingham fluid
e_{min}	minimum void ratio of sand	μ	apparent viscosity (mPa s) = τ/γ
e_{max}	maximum void ratio of sand	μ_{eq}	apparent viscosity at equilibrium (mPa s)
FC	non-plastic silts content by dry weight of soil (%)	μ_r	the relative viscosity ($=\mu_{eq,grout}/\mu_{water}$)
Gs	specific gravity	$\phi_1, \phi_2, \phi_3, \phi_4$ and ϕ_5	empirical constants for the proposed groutability, N^*

ell (1993) showed that cement-based grouts with the same w/c ratios, but with different amount of super-plasticizer, resulted in significantly different penetration distances. This change was attributed to the fact that the super-plasticizer changes the rheological properties of the cement-based grouts affecting its permeation through soils. Thus, the rheological properties of grouts should be incorporated into the groutability criterion of granular soils rather than the weight ratios. The rheological parameters of grouts such as yield stress and apparent viscosity can be measured through rheological tests. Yield stress controls the stoppage of grout flow and thus, constraining the propagation of grouts through soils (Axelsson et al., 2008; Axelsson et al., 2009). Yield Stress is also the parameter used to estimate the post grouting stability (Cambefort, 1977). The apparent viscosity describes the total resistance of grouts to flow through granular soils, which is related to the flow rate (De Paoli et al., 1992a).

This study presents an attempt to link the rheological parameters of chemically modified bentonite suspensions to groutability of granular soils. The rheology of concentrated bentonite suspensions are modified by using an ionic additive, sodium pyrophosphate (SPP). The sodium pyrophosphate was chosen because it displays pronounced dispersing capability (Penner and Lagaly, 2001; Tchillingarian, 1952) as well as retaining the time dependent buildup in rheological parameters, both of which are desirable properties as a grout; the “increasing mobility” effect of an additive need to be temporary so that the suspensions would start gelling gradually over time to achieve the resistance to wash-out and settling after permeation. This paper focuses on the effect of change in initial mobility of SPP modified suspensions on groutability of sand. Two rheological parameters (yield stress and apparent viscosity) are used to evaluate initial mobility and correlate it to the pore volume of injected suspensions. The effect of other experimental parameters on the suspension flow such as effective grain size, relative density, fines content and injection pressure are also investigated and correlated in a similar way to the rheological parameters. Based on the correlations of each parameter to the injected pore volumes of the suspensions, a new groutability criterion for granular soils using the SPP modified bentonite grouts is proposed.

2. Experimental program

2.1. Materials

Four different sands with different effective grain size (D_{10}), which provides the applicable range of hydraulic conductivity for particulate grouts ($k > 10^{-2}$ cm/s based on recommendations by Karol (2003)), were used in this study. All sands were classified as a SP based on a USCS classification. Table 1 summarizes the index properties of the tested sands based on ASTM standards. Wyoming sodium-bentonite (CP-200, CETCO) was used to prepare the suspensions. The bentonite particles are platy-like in shape and usually less than 1 or 2 μm in size (Luckham and Rossi, 1999; Mitchell, 1993). The raw bentonite was screened through a No. 200 sieve to minimize the impurities such as plagioclase feldspar, orthoclase, and muscovite minerals (Abend and Lagaly, 2000; Clarke, 2008). This process produced approximately 95% of particles less than 25 μm and 50% of particles less than 1 μm . No further purification and/or gradation were applied to simulate the expected process for mass production of material for field applications. The physical properties of the sieved bentonite are summarized in Table 2. The grain size distribution curves for the tested sands and sieved bentonite are shown in Fig. 1.

Since Na/Ca ratio is the critical parameter affecting rheological properties of bentonite suspensions (Brandenburg and Lagaly, 1988), the chemical analysis was performed using Philips/FEI XL30 Environmental Scanning Electron Microscope (ESEM) equipped with energy diffraction analysis of X-ray (EDX) to characterize chemical composition of the sieved bentonite powder. A Gaseous Secondary Electron (GSE) detector was utilized with frame and spot mode of EDX. The molar ratio of the sieved bentonite was 1.9. The chemical components of bentonite are presented in Table 3.

The pH of Bentonite suspensions was measured using JENCO 60 pH meter and showed strong alkalinity with an average pH of 9.3, standard deviation and the coefficient of variation (COV) of 0.3 and 0.03, respectively. Kelessidis et al. (2007) reported that for concentrated bentonite suspensions (6.42% by weight), with pH values beyond the natural pH (approximately 9.0), there was little difference

Table 1
Index properties of the tested sands.

Sand	G _s ^a	e _{max} ^b	e _{min} ^c	D ₁₀ (mm) ^d	D ₃₀ (mm) ^d	D ₆₀ (mm) ^d	Cu	Cc	USCS
Ottawa C778	2.65	0.76	0.50	0.20	0.32	0.40	1.94	1.28	SP
Monterey #0/30	2.64	0.85	0.57	0.31	0.46	0.59	1.92	1.13	SP
Aggregate	2.68	0.64	0.43	0.28	0.48	0.94	3.36	0.88	SP
Nevada	2.67	0.89	0.51	0.12	0.16	0.23	1.97	0.89	SP

^a ASTM D854-02.

^b D 4254.

^c D 4253.

^d D 422-63.

Table 2
Physical properties of Wyoming bentonite (CP-200).

Plastic limit	38%	Cation exchange capacity ^a	91 meq/100 g
Liquid limit	440%	Specific area ^b	712 m ² /g
Specific gravity (G _s)	2.7	pH	9.3
Initial water content	8.3%	Swelling capacity	16 ml/2 g

^a Methylene blue adsorption test.

^b Calculated the method suggested by Santamarina et al. (2002).

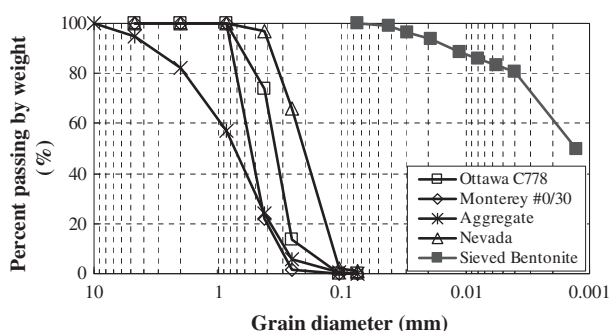


Fig. 1. Grain size distribution curves for the tested sands and sieved bentonite.

of pH values between the moment of mixing and full hydration (16 h). In addition, Clarke (2008) reported that the pH of the SPP modified suspensions did not significantly vary with the resting time and SPP concentrations. Based on these observations, the effect of pH on rheological properties of bentonite suspensions was considered minimal and ignored throughout this study. The cation exchange capacity and specific surface area were determined by the methylene blue (MB) adsorption technique. The chemical formula and molecular weight of methylene blue were C₁₆H₁₈ClN₃·S·3H₂O and 373.90, respectively. Methylene blue, which is the dissociated cationic dye (C₁₆H₁₈ClN₃⁺) in aqueous solution, replaces base cations (Na⁺, K⁺, Ca²⁺ and Mg²⁺) of clay minerals in an irreversible manner and covers the particle surfaces so that both cation exchange capacity and specific surface area can be estimated based on the amount of adsorbed methylene blue dye. The surface area covered by methylene blue molecule was assumed to be 130 Å² (see Table 3).

Table 3
Chemical analysis of Wyoming bentonite (CP-200), wt.%.

O	53.05	K	0.52
Na	2.27	Ca	1.2
Mg	1.52	Ti	0.15
Al	9.07	Cr	0.11
Si	28.77	Mn	0.2
P	0.46	Fe	2.31
S	0.43	Total	100
Cl	0.09	Na/Ca	1.9

Commercially available Sodium pyrophosphate decahydrated (Na₄P₂O₇·10H₂O) was utilized in this study. Specific gravity and molecular weight of the chemical were 1.8 and 446.06, respectively. Since the amount of SPP needed for each batch was very small, a 5% SPP solution was prepared in advance and the appropriate amount of solution was added to the water and bentonite to increase the accuracy of the measurements. The average pH of the 5% SPP solution was 9.5. De-ionized water with constant ionic concentration of 2 × 10⁻⁵ mM was used for preparing all the bentonite suspensions and SPP solution. A non-plastic silt (PI = 16.5%, LL = 49% and the average particle size of 13.5 μm) was mixed with the different sands to prepare specimens with various fines content.

2.2. Test equipment and procedures

2.2.1. Rheological test

A Physica MCR 301 rheometer was utilized in this study to perform all the rheological tests on the bentonite suspensions. The vane geometry was selected since it can minimize the effects of disturbance (from sample loading) and wall slip (during shearing) on the measured yield stress (Barnes and Carnali, 1990; Barnes and Nguyen, 2001; Cheng, 1986; Keentok, 1982; Stokes and Telford, 2004). In addition, yield stress (or cohesion) measurement using vane geometry has been a standard method of field quality control for high mobility grouts (Chuaqui and Bruce, 2003). The vane used was a six-bladed vane, each blade having a thickness of 1 mm and a length of 16 mm. The radius of the vane was 11 mm, resulting in a 3.46 mm of gap between the cup and the vane. Sample volume was maintained at 37 ml, which allows the vane to penetrate approximately twice its depth into the suspension. The cups manufactured for long term resting of samples were 80 mm in length and 29 mm in internal diameter. No surface treatment, such as sand blasting on the surface of cup or vane, was applied. The end effect of the vane was considered small enough to be ignored for practical purposes (Barnes and Carnali, 1990). All tests were performed at a temperature of 22° (±0.03°); the temperature was controlled using the built in Peltier temperature control system in the rheometer.

The screened bentonite powder was mixed with de-ionized water; the weight fraction of bentonite suspension was calculated as the weight ratio of bentonite to the total weight of suspension. In the calculation of bentonite fraction, the water content of the bentonite in its storing conditions was accounted for in calculating the weight of the dry bentonite. The concentration of SPP was calculated as the weight ratio of SPP to the dry weight of bentonite. The mixing process of the bentonite suspensions included three steps; each step consisted of 5 min of high shear mixing of the suspensions followed by manual scraping of the sides and base of the mixing cup to remove any attached bentonite flocs. The mixing procedure greatly affects the rheological properties of the bentonite suspensions, particularly, the sequence of adding the SPP. In

this study, the 5% SPP solution was mixed with bentonite and water without any resting periods for immediate application of bentonite suspensions in the field. For samples rested for extended periods of time before testing, the suspensions were poured into cups manufactured specifically for this study. The cups were identical in size to the cup used for the vane tests in the rheometer. A layer of mineral oil was added to the top of the bentonite suspensions to reduce any evaporation from the samples, and then the cups were tightly sealed afterwards and stored away.

The typical method to measure yield stress using the vane geometry is the constant shear rate technique; this method directly estimates yield stress as a peak stress in torque-time response at a constant shear rate. The torsional strain is increased at a constant but sufficiently slow rate and the change in torque is monitored with time, and then the peak stress is determined as the yield stress. The advantage of this method is that yield stress can be obtained by a direct measurement without any subjective interpretation (Barnes and Nguyen, 2001). However, the measured yield stress is highly dependent on the applied shear rates (Barnes and Nguyen, 2001; Bekkour et al., 2005; Dzuy and Boger, 1983; Saak et al., 2001) and particle fractions (Barnes and Nguyen, 2001). Barnes and Nguyen (2001) suggested that this method is the most appropriate for yield stresses greater than 10 Pa. Since the tested suspensions with low fractions of bentonite and/or high percentages of SPP have yield stresses lower than 10 Pa, the stress ramp method was selected for this study over the constant shear rate method (Clarke, 2008; Zhu et al., 2001). The stress ramp method can be used to measure yield stresses below 10 Pa, and was considered to be a consistent way of measuring low and high yield stresses.

The stress ramp technique is a stress-controlled test in which the shear stress levels are increased incrementally. In this study, each stress level was maintained for 12 s and the data was recorded at the end of each interval. The tests were programmed such that samples were rested for 2 min after inserting the vane to provide a consistent initial condition (in both immediately after mixing and the time dependent measurements). Yield stress in this technique is typically determined by fitting constitutive models such as Bingham and Herschel-Bulkley, and Casson to the data. However, the yield stress obtained from the models tends to be an overestimate compared to the actual yield stress (Coussot, 2005) and may not have any physical meaning (Zhu et al., 2001). As an alternative, the yield stress can be graphically measured from the shear stress (τ) – shear strain (γ) plots. This approach utilizes either a τ - $\log \gamma$ or a $\log \tau$ - $\log \gamma$ plot (Clarke, 2008; Zhu et al., 2001); all yield stresses in this study was determined based on a $\log \tau$ - $\log \gamma$ plot. An example of this graphical method for 10% bentonite suspension is shown in Fig. 2. Initially, the stress-strain curve displays a solid-like response (linear increase in stress with increasing strain) followed by a significant increase in strain with minimal change in shear stresses when the yield stress value is exceeded (liquid like response).

The ramp rate is one of the important factors affecting yield stress measurement using the stress ramp technique. Zhu et al. (2001) suggested that slow enough ramp rates should be used in this technique and reported a little difference (5%) in yield stress measurement of 60% TiO₂ suspensions with three different rates of 0.063, 0.1 and 0.13 Pa s⁻¹. To investigate the ramp rate effects on the measured yield stress in bentonite suspensions, two sets of tests were performed on 5% and 7.5% suspensions immediately after mixing as shown in Fig. 3. The 5% suspensions were tested at ramp rates of 0.5 and 1 Pa/step (0.042 and 0.083 Pa s⁻¹); the two rates resulted in similar yield stresses. For the 7.5% suspensions, the tests were performed at the ramp rates of 1, 2 and 3 Pa/step (0.083, 0.167 and 0.25 Pa s⁻¹). The three different ramp rates produced an average yield stress of 27.9 Pa (± 0.3 Pa), indicat-

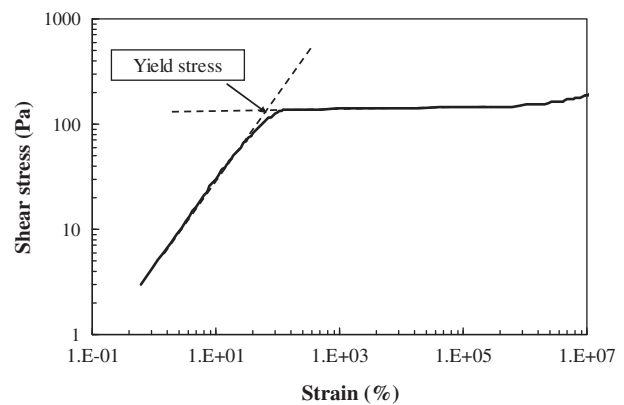


Fig. 2. Example of determining yield stress in stress ramp technique: 10% bentonite suspension.

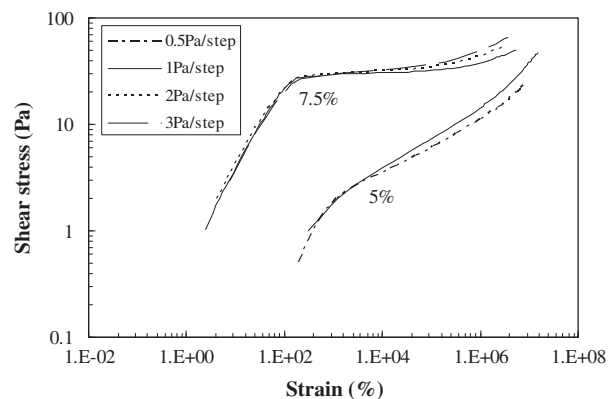


Fig. 3. Comparison of different ramp rates of (a) 0.5 and 1 Pa/step for 5% bentonite suspensions, and (b) 1, 2 and 3 Pa/step for 7.5% bentonite suspensions.

ing that the differences in these rates are small enough to ignore. Applying a slow ramp rate becomes impractical and can result in inaccurate measurements, especially when the suspensions have high yield stress. A slow ramp rate leads to long testing times, resulting in possible change in yield stress due to thixotropy (particularly in “immediately after mixing” tests) and drying out of specimens in all tests. Based on these results, the ramp rate of 1 Pa/step (0.083 Pa s⁻¹) was used for low strength suspensions (lower bentonite fractions, higher SPP concentrations, and/or at early times) to improve the accuracy of the measured yield stresses; 3 Pa/step (0.25 Pa s⁻¹) was used for stronger grouts to decrease the time required to reach the yield stress and minimize sample evaporation during the tests.

Accurate measurement of apparent viscosity in bentonite suspensions with stress ramp technique is also challenging because two parameters (shear rate and time) changes simultaneously during testing. Furthermore, the initial shear rate is highly dependent on the stress applied. However, as shown in Fig. 4, this effect diminished at high shear rates and reaches a steady state (or equilibrium state), producing essentially constant apparent viscosities. Since the apparent viscosity at high shear rates is more important than that at low shear rates when analyzing the injection process (Markou and Atmatzidis, 2002), it was considered appropriate to use the apparent viscosities at the equilibrium state. This selection of apparent viscosity could remove the shear rate dependency in apparent viscosity and allowed one point comparison to study its effect on the groutability. However, an inertia effect was observed for the diluted suspensions and suspensions with high percentage

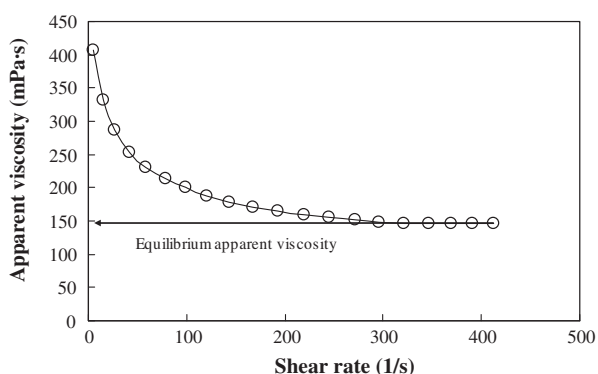


Fig. 4. Determination of apparent viscosity at equilibrium: 10% bentonite suspension with 2% SPP.

of SPP; apparent viscosity for the diluted suspensions decreased up to a shear rate of approximately 250 s^{-1} , and then started slightly increasing at higher shear rates. In this case, the minimum apparent viscosity at high shear rate was selected as the equilibrium apparent viscosity.

2.2.2. 1-D injection test

Although the 1-D injection tests in laboratory underestimates the filtration effects (Mittag and Salvidis, 2003) and does not reflect multistage injection as typically performed in the field (Santagata and Santagata, 2003), it has been a conventional technique conducted in laboratory to investigate groutability and penetrability in granular soils. A schematic of the injection test setup used in this study is depicted in Fig. 5. The permeation cell was transparent and had a 3.8 cm internal diameter and a 21 cm height. Clean sands were carefully air pluviated with a funnel into the permeation cell. The free drop height was adjusted to achieve the desired relative densities; for the dense specimens, the permeation cell was tapped on the sides to decrease the void ratio to the target values. For the sands including fines, the clean sands were initially mixed with designated amounts of fines (5%, 10% and 15% by dry weight of sand) while being sprayed with water, followed by hand compaction (moisture tamping method) to produce the similar skeletal relative density (30% or 80%) to those prepared without fines. Hwang (2010) reported that this process could produce relatively uniform specimens compared to the air pluviation with dry mixtures. The specimens were then slowly flushed with water from the bottom to the top not to cause any fine washing through the specimens. A filter material, consisting of a 25 mm thick layer of coarse sand ($1.2\text{ mm} < D < 1.7\text{ mm}$) and a 25 mm thick layer of

pea gravel ($D > 4.75\text{ mm}$), was placed on the top and bottom of the sand column to help produce a uniform supply of bentonite suspensions throughout the cross-section of the sand column.

The air-pluviated sand columns were initially saturated with slow flushing of de-aired water (at least 3 pore volumes) from bottom to top, and then more pore volume of water (at least 3 pore volumes) was flushed at a pressure of 35 kPa to remove air bubbles in the specimen (ASTM D4320/D4320M-09).

According to Perret et al. (2000), partially saturated sands showed a faster propagation compared to that in fully saturated sands due to the suction created by negative pore water pressure. However, the effect of degree of saturation in penetration of grout was not considered through this study by performing all the tests at nearly saturated condition. While the actual degree of saturation of the individual specimens was not measured in this study, the measured hydraulic conductivity of the sand columns resulted in $\pm 25\%$ from the reference hydraulic conductivity of the tested sands (measured in the fully saturated condition), indicating the high degree of saturation.

Bentonite suspensions were placed into a pressure cell within 2 min after mixing for consistency with rheological tests. The bentonite suspensions were injected into the sand columns using a pressure panel at the constant pressures of 35 and 140 kPa. A balance was placed to measure weight of effluents during testing. The volume of effluent water was considered the same as the volume of the injected suspensions. The grout intake in the sand was corrected by considering the pore volumes of the filter layers since the grout intake includes the amount of intake through the filter layer, and the corrected grout intake was normalized with the pore volume of the sand column for consistent comparison between different experimental parameters without having any effects from different porosities.

There is no consensus on how to determine a successful grouting since it varies with types of grouts, field conditions and performance of the grouted soil. Ozgurel and Vipulanandan (2005) considered a successful grouting in chemical grouts (acrylamide) if the injected volume of grouts was reached 1 pore volume at 140 kPa after 8 min. Markou and Atmatzidis (2002) utilized the criterion of 2 pore volume or the limiting pressure of 350 kPa at the constant flow rate of 60 l/h for fly ash grouts. Moreover, Mittag and Salvidis, 2003 introduced the German criterion of 3 pore volumes at 600 kPa for constant flow rate tests of micro-fine cement grouts, on samples with a height to diameter ratio greater than 4. In this study, the successful grouting was considered if at least 1 pore volume could be injected at the pressure of 140 kPa within 10 min. This criterion was selected based on the similarity of injection technique (constant pressure) to what Ozgurel and Vipulanandan (2005) used and to utilize low level of injection pressures.

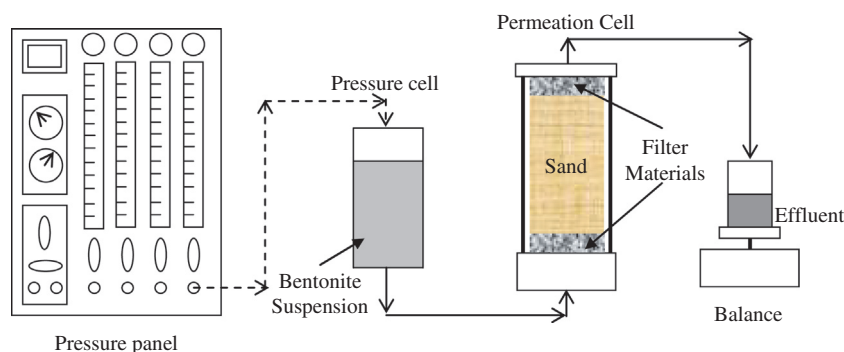


Fig. 5. Schematic of constant pressure injection test setup (the dashed and solid lines represent a flow of air-pressure and liquid respectively).

3. Results and discussion

3.1. Rheological parameters

The variation of yield stress with bentonite fraction at different SPP concentrations is presented in Fig. 6. All the reported rheological properties in this paper are the average of at least three measurements on three different samples; the measured properties from the different samples were similar with a COVs ranging from 0.01 to 0.2. The average yield stresses increased exponentially with the increase of bentonite fraction, indicating that yield stress is a function of particle fractions (similar trends were reported by Dzu and Boger (1983) and Mahaut et al. (2008)). Bentonite suspensions with the high solid fractions have more network structures which govern its yield behavior. SPP disrupts the formation of networks so that the yield stress starts decreasing with the addition of SPP. Yield stress at 7.5%, 10%, and 12% decreased significantly from 27.9, 137.5 and 457.1 to approximately zero at SPP concentration of 2%, 3%, and 4%, respectively. For all suspensions that did not show a yield stress, the minimum ramp stress step of 1 Pa was assigned. These results imply that the SPP can limit the buildup of yield stress. The modified bentonite suspensions showed similar exponential increase in yield stress as observed in the unmodified ones. The bentonite swelling would affect the yield stress measurements, especially for the “unmodified” suspensions. After mixing, the adsorption of water molecules between the interlayers of the clay platelets causes swelling of the bentonite (Luckham and Rossi, 1999); this swelling produces higher repulsive forces that weaken the structures formed by the delaminated platelets. The resulting weak structures are easy to separate under shearing, and therefore, reduce the yield stress. However, this effect becomes minimal for the modified suspensions where the repulsive forces were much higher than those in the unmodified suspensions due to the presence of the negative phosphate anions.

In Fig. 7, the variation of apparent viscosity (at the equilibrium state) with bentonite fraction and SPP concentration is presented. The apparent viscosity increased with an increase of bentonite fraction, and decreased with increasing SPP concentration. The apparent viscosities were reduced by approximately 50% for 7.5%, 10% and 12% suspensions with 2%, 3% and 4% SPP, respectively. Moreover, the SPP dosage did not show any coagulation, indicating that the amount of SPP was still less than the critical coagulation concentration (the concentration of an ion where coagulation induces (Penner and Lagaly, 2001)). This implies that the size of bentonite particles will not vary with the SPP modification, and thus, maintaining the effect of the physical properties of bentonite particles (shape and particle size) on the groutability. Although the

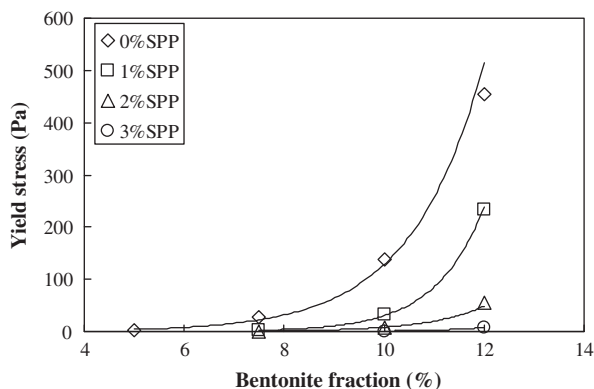


Fig. 6. Yield stress at the bentonite fractions of 5%, 7.5%, 10%, and 12% with 0%, 1%, 2% and 3% SPP.

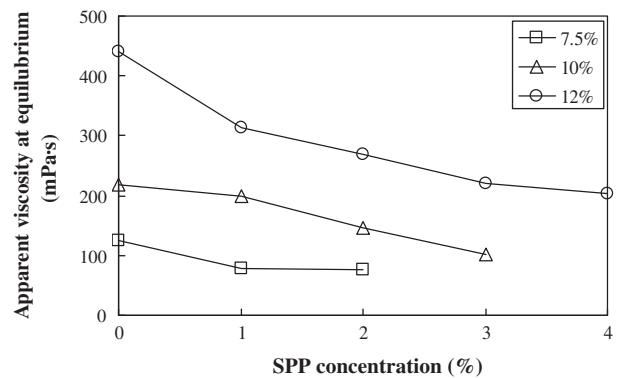


Fig. 7. Apparent viscosity (at equilibrium state) of 7.5%, 10%, and 12% bentonite suspensions with 0–4% SPP.

“effective” particle size of the bentonite can be increased due to the attached water to the surface of the bentonite as part of the diffused double layer, this “effective” larger grain size is dependent on the various factors (pH, ionic strength of water, type of cations) that affect rheological properties of the bentonite suspensions since those parameters control the inter-particle forces and thus the resulting structures within the suspension. Therefore, using the actual grain size of the bentonite is necessary to capture the baseline geometrical clogging that could occur while the double layer is accounted for in the rheological properties. Because of the weak structures in the bentonite suspensions formed by bentonite swelling, the apparent viscosity is slightly reduced at low shear rates, but the effect becomes minimal for the modified suspensions and high shear rates due to the high repulsive and shearing forces, respectively. Moreover, the change in the apparent viscosity from 1% SPP to 2% SPP at 7.5% suspension resulted in only 3% difference, indicating that the effect of SPP on the apparent viscosity is minimal beyond a threshold percentage of SPP. Based on these observations, the SPP concentrations of 1%, 3% and 4% for 7.5%, 10% and 12% suspensions were mainly utilized through this study as an upper bound dosage of SPP.

3.2. Injection tests

The bentonite suspensions (both, modified and unmodified) were injected into sand columns prepared at various conditions to investigate the effect of sand effective grain size (D_{10}), relative density (D_r), fines content (FC), and injection pressures (P) on injected pore volume of suspensions. This section presents the relationship between each soil/grout properties and injected pore volume of the bentonite suspensions.

Fig. 8 shows the injected pore volume versus the yield stress of the bentonite suspensions. The unmodified suspensions exhibited a significant reduction in the injected pore volumes with the decrease in yield stress. As the yield stress increases from 3.4 Pa to 471 Pa, the injected pore volume decreased from 1.5 to 0.1 pore volume. The 7.5% suspension with 1% SPP produced 1.5 times larger injected pore volume than the unmodified suspension. On the other hand, the injected pore volume in the 10% and 12% suspensions with 3% and 4% SPP increased 1.8 and 2.6 times, respectively, compared to those of the unmodified suspensions. For the same bentonite fraction, a reduction in yield stress produced consistently higher injected pore volumes. However, the increase in the injected pore volume of the modified suspensions showed a dependency on particle fractions at the similar yield stresses and therefore, there is no unique relationship between yield stress and injected pore volume, even for one given material.

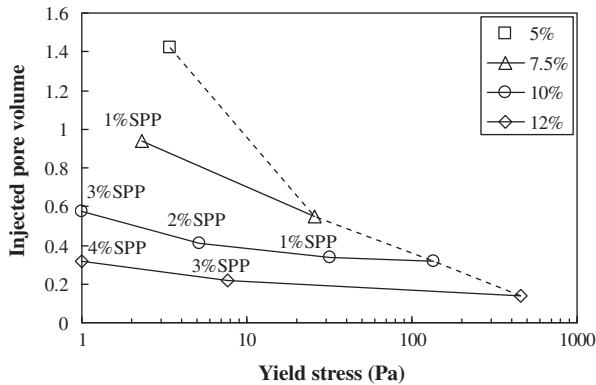


Fig. 8. Injected pore volume based on yield stresses of various bentonite suspensions at $D_{10} = 0.2$ mm, $Dr = 30\%$ and $P = 35$ kPa (the dashed line is for the unmodified grouts and the solid lines are for the modified suspensions).

According to de Paoli et al. (1992a), the flow resistance of a grout at a given shear rate consists of two components, yield and viscous (plastic viscosity). Even when a grout is flowing (the apparent shear rate is greater than zero), there is still a contribution of yield stress to the flow resistance by providing additional drag forces. This implies that neither the yield nor the viscous component is able to fully capture the volumetric response of the grout. In order to consider both effects, the apparent viscosity, which includes both parameters, was correlated to the injected pore volume. Fig. 9 displays the relationship between the equilibrium apparent viscosity and injected pore volume. As the apparent viscosity increased, the injected pore volume in both the unmodified and modified suspensions consistently decreased with a power function regardless of bentonite fractions.

In the case of the unmodified suspensions, the effect of yield component (due to the flocculated network structures) under flow condition on the apparent viscosity is dominant, resulting in consistent reduction in the injected pore volume with the reduction in yield stress. On the other hand, the contribution of the viscous component in the apparent viscosity becomes dominant in the modified suspensions. While the yield component is reduced in the modified suspensions due to the disruption of network formation by SPP, the presence of large amounts of particles produces a high viscous component. Coussot (2005) showed that the viscous component is more dependent on the particle fractions than the network structures. Therefore, the modified suspensions with higher bentonite fractions exhibit more viscous resistance than those with low bentonite fractions at the similar level of low yield

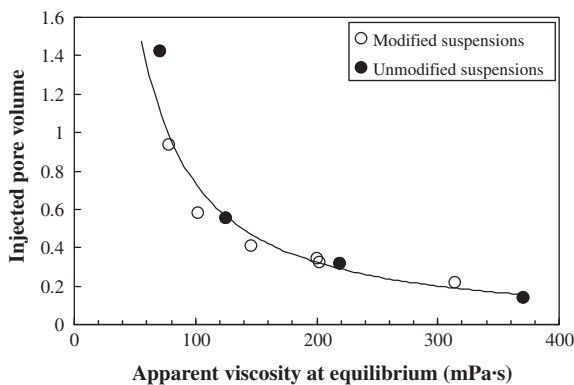


Fig. 9. Injected pore volume based on equilibrium apparent viscosities of the unmodified and modified bentonite suspensions at $D_{10} = 0.20$ mm, $Dr = 30\%$ and $P = 35$ kPa.

stress. As a result, the suspension flows with lower flow rates, leading to a smaller injected pore volume. This is consistent with the results presented in Fig. 9; for suspensions with similar yield stress, the suspensions with higher bentonite fraction had the smaller injected pore volume. It should be noted that with higher bentonite concentrations, filtration becomes a critical factor in addition to the change in rheological properties of suspensions. Even though the SPP treatment may reduce the degree of filtration (Kim and Whittle, 2009), for the high fractions of bentonite particles, some degree of filtration is still expected.

Similar to cement-based grouts, the groutability of granular soils, with any suspension type grout, varies with the pore sizes of the soil. As the effective grain size (D_{10}) increases, pore spaces where the suspension can flow increase, resulting in an increased injected pore volume. Fig. 10 shows injected pore volumes of 12% bentonite suspensions with 4% SPP through sands with different effective grain sizes. The injected pore volume of the suspensions increased exponentially with an increase in effective grain size of the soils, indicating an increase in the possibility of injection with an increase in the effective grain size of soils (D_{10}). Similar effect has been reported in literatures (Akbulut and Saglamer, 2002; Santagata and Santagata, 2003; Ozgurel and Vipulanandan, 2005) on chemical and cement-based grouts. While the suspensions could not be injected up to 1 pore volume through Nevada and Ottawa sand ($D_{10} = 0.14$ and 0.2 mm, respectively), they could be injected over 1 pore volume through aggregate and Monterey #30 sand ($D_{10} = 0.28$ and 31 mm, respectively).

Grout intake at relative densities of 30% and 80% under 35 kPa grouting pressure are compared in Fig. 11a. The loose specimens (relative density of 30%) produced higher initial flow rates than the dense specimens (relative density of 80%), but the difference in the amount of injected suspensions into the dense and loose specimens varied with the fractions of bentonite. While the 7.5% suspensions showed a larger grout intake in the dense soil (approximately 30%), the difference between the grout intake measured at the two relative densities decreased as the bentonite fractions increased. This may be attributed to an increase in the creep flow (additional filling of voids which occurs after the initial penetration of the grouts) due to a decreased filtration in the dense specimens, leading to a lower difference in the final grout intakes despite of the reduction in initial penetration (Axelsson et al., 2009). The creep flow was more prominent in the dense specimen permeated with 7.5% suspension resulting in even more grout intake in the dense specimen than in the loose specimen. Fig. 11(b) shows the injected pore volumes of suspensions into the loose and dense sands relative to each other; the injected pore volumes were relatively identical in the 10% and 12% suspensions with 3%

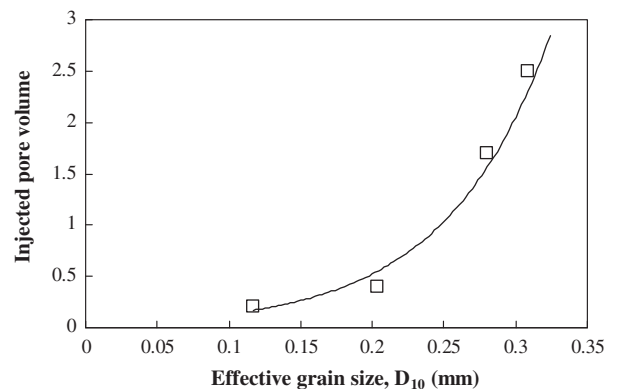
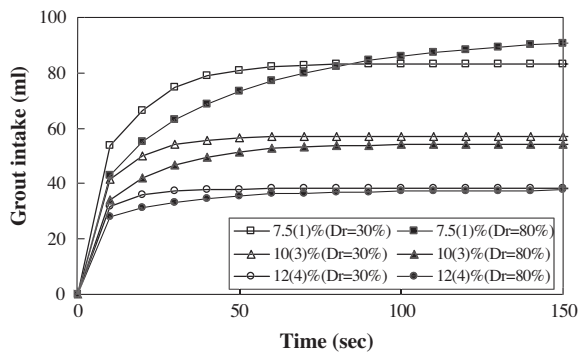
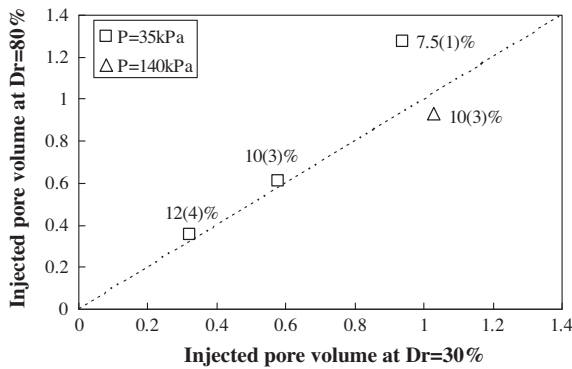


Fig. 10. Injected pore volume based on effective grain sizes of sands at ($\mu_{eq} = 203$ - mPa s, yield stress <1 Pa, $Dr = 30\%$ and $P = 140$ kPa).



(a) Grout intake versus time under 35 kPa pressure



(b) Injected pore volume at Dr=80% versus Dr=30%

Fig. 11. (a) Grout intake at 35 kPa injection pressure and (b) injected pore volume based on relative density of sands at 7.5(1)%, 10(3)%, 12(4)% bentonite suspensions, $D_{10} = 0.20$ mm (the numbers next to the data points indicated the bentonite content and the SPP concentration is added in the parenthesis).

and 4% SPP, respectively, and slightly increased in the 7.5% suspensions with 1% SPP with the increase in the relative density. It should be noted that the reduction in the porosity of the sand column with higher density resulted in approximately 10% increase in injected pore volume for the same grout intake in a loose sand column.

Since the injection pressure of 35 kPa was not enough to differentiate the effect of relative density in the concentrated suspensions, the 10% suspensions with 3% SPP was injected with the higher pressure of 140 kPa. The injected pore volume for both densities increased by approximately 60%; however, the difference in the injected pore volumes between sands with different densities was small (approximately 10%, Fig. 11b). Based on these observations, it was concluded that the overall effect of relative density on the injected pore volume at a constant injection pressure was small compared to other parameters such as the rheological parameters and effective grain size.

For field application, the effect of fines content on groutability should be evaluated since the sand in the field typically includes some portion of low plasticity silts. Fig. 12 depicts the effect of fines content on the injected pore volumes; the injected pore volume of the suspensions decreased exponentially with an increase of fines content in sand columns. Ozgurel and Vipulanandan (2005) reported a high non-linearity of injection pressure depending on fines content with a chemical grout (acrylamide). The sand column with 5% fines did not show any significant reduction in the injected pore volume, indicating that the soils which have less than 5% fines will have the same groutability as clean sand. Soils with fines contents greater than 20% may not be groutable with particulate grouting (Karol, 2003).

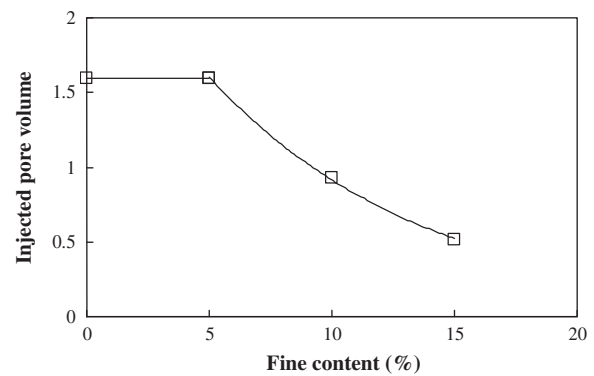


Fig. 12. Injected pore volume based on fine contents of 0%, 5%, 10%, and 15% (by weight of dry sand) at $\mu_{eq} = 78.1$ mPa s, yield stress = 2.3 Pa, $D_0 = 0.2$ mm, $Dr_{skel-tal} = 30\%$, and $P = 140$ kPa.

Two injection pressures (35 and 140 kPa) were utilized to investigate the effect of injection pressure on groutability. A higher injection pressure was required to achieve more injected pore volumes under some of the sand columns testing conditions (small effective grain size and high relative density and fines content). However, increasing injection pressure beyond 140 kPa could induce movement of soil grains, resulting in disturbance the soil's structure (Rugg, 2010). The injected pore volumes at 140 kPa and those at 35 kPa are compared in Fig. 13. As the injection pressure increased, the injected pore volume increased approximately 1.4–1.8 times. The increase in injected pore volume was not uniformly proportional to the increase in applied pressure possibly due to filtration, which is a function of particle fractions. The filtration process may be promoted by separation of particles and water and accelerated by pressures (Akbulut and Saglamer, 2002), forming filter cakes near the injection point.

3.3. New groutability for the modified bentonite suspensions

A new groutability criterion for bentonite suspension was developed using the relationships observed between injected pore volume and the different sand and grout parameters discussed in the previous section. The proposed groutability criterion includes similar parameters (grain size of sand and grouts, injection pressure, fines content, and relative density) to that proposed by Akbulut and Saglamer (2002). However, the new criterion includes the rheological parameter rather than weight ratios of the grout. The summarized step by step procedures include: (1) selection of the global model (Eq. (1)), (2) determination of model parameters, (3) development of a groutability equation, (4) calibration of equation constants, and (5) determination of successful grouting based on the injected pore volumes. Initially, the injected pore volume and groutability were correlated using a power function since apparent viscosity showed a dominant effect on injected pore volume (Fig. 9). Using the measured pore volumes, the model coefficients were found by regression analyses, controlling the target range of groutability ($N^* = 0-15$) on trial and error basis to produce a similar range of groutability to the existing criteria ($N = 10-25$) for comparison purposes. Within the range, the injected pore volume has a perfect correlation ($R^2 = 1$) with the target groutability. By using the estimated groutability number, the empirical constants in Eq. (2) were calculated using root mean square error method.

$$IPv = C \times N^{*n} \quad (1)$$

where IPv is the injected pore volume of grouts, N^* is the target groutability of bentonite suspension, C and n are the empirical con-

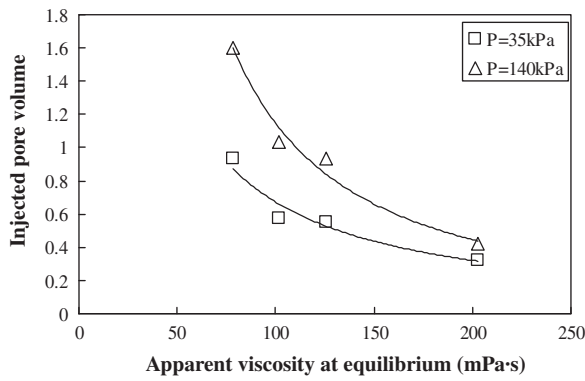


Fig. 13. Injected pore volume based on injection pressure: 7.5%, 7.5(1)%, 10(3)%, 12(4)% bentonite suspensions (the numbers in the parenthesis are the concentration of SPP).

Table 4
Empirical parameters proposed in this study.

Empirical parameters	ϕ_1	ϕ_2	ϕ_3	ϕ_4	ϕ_5
	1900	0.2	1.4	8.5	9.3

stants, estimated to be 2.2×10^{-4} and 3.5 respectively. The calculated groutability (N^*) was plotted with each parameter (effective grain size, relative density, fines content, apparent viscosity, and injection pressures), producing a function of the form $N^* = -f(N_c) + f(P/\mu) + f(Dr) + f(FC)$. Based on this function, an empirical equation to estimate groutability considering how it is affected by each component was proposed as follows:

$$N^* = N_c + \phi_1 \frac{(P/1atm)^{\phi_2}}{(\mu_r)^{\phi_3}} + \left(\frac{Dr}{100}\right)^{\phi_4} - EXP\left(\phi_5 \frac{FC}{100}\right) \quad (2)$$

where N^* is the groutability of bentonite suspensions, $\phi_1, \phi_2, \phi_3, \phi_4$ and ϕ_5 are the empirical constants, P is the injection pressure (kPa), μ_r is the relative apparent viscosity ($\mu_{grout} \text{ (mPa s)} / \mu_{water} \text{ (mPa s)}$), FC is the non-plastic fines content in granular soils (%), N_c is the **Burwell's (1958)** second groutability ratio ($D_{10,sand} \text{ (mm)} / d_{95,bentonite} \text{ (mm)}$). All factors affecting groutability were normalized to obtain a dimensionless number. The empirical constants were determined by correlating the calculated groutability to the proposed equation using a root mean square error method. **Table 4** summarizes the empirical parameters determined by the regression analysis. It should be noted that the correlation should be interpreted with the interactive effect between parameters since the penetration of grout through soil does not rely on one single parameter. For instance, soil having high relative density tended to increase the injected pore volumes at the pressure of 35 kPa, but it was still required to use the higher injection pressure and lower viscosity suspensions than the soils having low relative density to achieve a successful grouting. Moreover, the proposed correlation is reasonable between the following intervals: $5 \leq \text{bentonite fraction} \leq 12\%$, $0 \leq \text{SPP} \leq 4\%$, $4.8 < N_c < 12.6$, $30 \leq Dr \leq 80\%$, $0 \leq FC \leq 15\%$, $k \geq 0.01 \text{ cm/s}$ and $P \leq 140 \text{ kPa}$. If the $N_c < 4.8$ and $FC > 20\%$, the bentonite suspensions did not penetrate into the soil and there was almost instantaneous stoppage even with very diluted suspensions (e.g. Nevada sand with 7.5% suspensions with 1% SPP at 140 kPa).

Fig. 14a shows the proposed correlation between groutability and the injected pore volumes. Since the proposed groutability is correlated to the injected pore volumes, a quantitative evaluation of successful grouting is possible based on the injected pore volumes (i.e. at least 1 Pv). Based on this criterion, it was found that a soil is “Groutable” if N^* was greater than 11, and “UngROUTable”

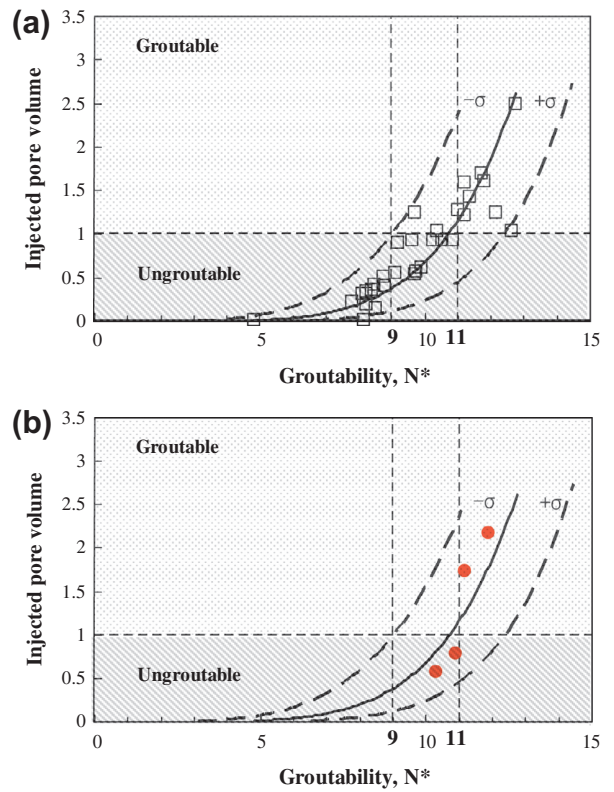


Fig. 14. (a) Proposed groutability criterion using the modified bentonite suspensions, and (b) groutability of different type of bentonite (Na/Ca = 5.1, $d_{95} = 25 \mu\text{m}$).

if N^* is less than 9. When the groutability lies within the 9 to 11 range, a trial grouting is recommended in the laboratory.

The proposed groutability criterion was tested with a different type of bentonite which has similar particle size ($d_{95} \approx 25 \mu\text{m}$), but the higher Na/Ca ratio (5 instead of 1.9). The different Na/Ca ratio implies that the bentonite suspensions will show different rheological properties from the original bentonite suspensions used to calibrate the proposed model. As the Na/Ca ratio increases, the yield stress and apparent viscosity of the unmodified 7.5% suspensions were significantly reduced, possibly due to the lack of Ca^{++} ions which exert attractive forces between bentonite particles (yield stresses of 26 and 10 Pa, apparent viscosities of 126 and 87 mPa s for the “original” and “new” suspensions, respectively) (**Brandenburg and Lagaly, 1988**). However, the modified suspensions displayed similar apparent viscosities since the degree of dispersion was essentially governed by the amount of phosphate anions and shear rates. The groutability was estimated based on the proposed equations with similar experimental conditions and using the same values of the empirical parameters presented in **Table 4**. **Fig. 14b** shows the groutability of the new bentonite versus the injected pore volume along with the proposed groutability criteria and mean and standard deviation of the results on the original bentonite. The new bentonite produced similar results to what was observed in the original bentonite, indicating that the proposed groutability criteria will be applicable for other type of bentonite suspensions as long as the rheological properties are correctly estimated.

3.4. Comparison with the existing criteria

The proposed groutability criterion was evaluated by comparing it with the existing criteria. The comparison of the proposed and the existing groutability is summarized in **Table 5**. The initial

Table 5
Comparison of groutability criteria for 32 tests.

Criteria	Groutable	UngROUTABLE	Number of predicted "Groutable" tests	Number of tests with injected pore volume >1
Burwell (1958)	>25	<11	30	11
Burwell (1958)*	>11	<5	8	6
Incecik and Ceran (1995)	>10	<10	30	11
This study**	>11	<9	9 (11)	9 (11)

** Data from New bentonite is not included except for numbers between brackets.
* When $d_{15,soil}/d_{85,grout} > 25$ and trial grouting at $5 < N < 11$.

estimation based on Burwell's (1958) criterion ($N = D_{15,soil}/d_{85,grout}$) produced N of 36, 50.9, 46.4 and 17.9 for Ottawa, Monterey #0/30, Aggregate and Nevada sand, respectively, regardless of the type of the grout mix, indicating that all 32 tests except for 2 tests on Nevada sand are groutable ($N > 25$). However, the injected pore volume was higher than 1 for only 11 out of these 30. The second criterion ($N = d_{10,soil}/d_{90,grout}$) produced N of 8.3, 12.6, 11.4 and 4.8 for Ottawa, Monterey #0/30, Aggregate and Nevada sand, respectively, determining only 8 data as groutable ($N > 11$). Out of these 8 tests, only 6 tests reached injected pore volumes in excess of 1. In addition, 5 tests could be injected over 1 pore volume with N values between 5 and 11. On the other hand, Incecik and Ceran (1995) criterion ($N = D_{10,soil}/d_{95,grout}$) estimated most of data (30 out of 32) as groutable ($N > 10$), but approximately 70% of data points could not be injected over 1 pore volume. The new proposed criteria was able to better predict the groutability of the sand even when including the 4 tests using the new bentonite that were not used to calibrate the model. The comparisons with the existing criteria indicate that the prediction of groutability using the existing groutability may cause inaccurate prediction of groutability in soils when the SPP modified bentonite suspensions are used in permeation grouting.

4. Conclusions

The rheological properties of the SPP modified bentonite suspensions were investigated to be incorporated in determining the rheological properties of the suspensions with groutability for granular soils. It was observed that the introduction of small amounts of sodium pyrophosphate (1–4% by dry weight of bentonite) could significantly reduce the yield stress and apparent viscosity of the bentonite suspensions, and therefore, increasing the injected pore volumes of suspensions.

While the yield stress did not produce a unique relationship with the injected pore volume (possibly due to different particle fractions in each bentonite suspension), the apparent viscosity showed a consistent relationship with the injected pore volumes. As apparent viscosity decreased, the injected volumes significantly increased. The injected pore volume was also influenced by other parameters such as the effective grain size, relative density, fines content and injection pressure. As the relative density and fines content decreased, the injected volumes increased; however, the effect of relative density was relatively small. On the other hand, the injected pore volume increased with an increase in the effective grain size of the grout and injection pressure. Based on the observed relationships between the injected pore volumes and experimental parameters (the properties of soil and bentonite suspensions, and injection pressure), a new groutability number for the modified bentonite suspensions was proposed. In addition,

the proposed groutability and a quantitative criterion suggests that soils are groutable when $N^* > 11$ and ungroutable when $N^* < 9$. For the soils exists between 9 and 11, trial grouting should be performed before field application. The proposed criterion was tested with different type of bentonite suspensions, resulting in similar trends to what observed in the proposed relationships.

The proposed criterion will be beneficial to evaluate groutability more accurately in granular soils using the SPP modified bentonite suspensions. This study showed a possible application of the modified bentonite suspensions in permeation grouting and the information from the proposed groutability may be helpful to design grouting works using the modified bentonite suspensions.

References

- Abend, S., Lagaly, G., 2000. Sol-gel transitions of sodium montmorillonite dispersions. *Appl. Clay Sci.* 16, 201–227.
- Akbulut, S., Saglam, A., 2002. Estimating the groutability of granular soils: a new approach. *Tunn. Under SP Technol.* 17 (4), 371–380.
- Axelsson, M., Gustafson, G., Fransson, Å., Funehag, J., 2008. Design criteria for permeation grouting in hard rock at great depths. In: *World Tunn Congr.-Underground Facilities for Better Environment and Safety, India*, pp. 510–520.
- Axelsson, M., Gustafson, G., Fransson, Å., 2009. Stop mechanism for cementitious grouts at different water-to-cement ratios. *Tunn. Undergr. Sp. Technol.* 24, 390–397.
- Barnes, H.A., Carnali, J.O., 1990. The vane-in-cup as a novel rheometer geometry for shear thinning and thixotropic materials. *J. Rheol.* 34, 841–867.
- Barnes, H.A., Nguyen, Q.D., 2001. Rotating vane rheometry a review. *J. Non-Newtonian Fluid Mech.* 98, 1–14.
- Bekkour, K., Leyama, M., Benchabane, A., Scrivener, O., 2005. Time-dependent rheological behavior of bentonite suspensions: an experimental study. *J. Rheol.* 49, 1329–1345.
- Bell, F.G., 1993. *Engineering Treatment of Soils*. E&FN Spon, London.
- Brandenburg, U., Lagaly, G., 1988. Rheological properties of sodium montmorillonite dispersions. *Appl. Clay Sci.* 3, 263–279.
- Burwell, E.B., 1958. Cement, clay grouting of foundations: practice of the corps of engineering. *J. Soil Mech. Foundation Div., ASCE* 84, 1551/1–1551/22.
- Cambefort, H., 1977. The principals and applications of grouting. *Q. J. Eng. Geol.* 10, 57–95.
- Chegbeleh, L.P., Nishigaki, M., Akudago, J.A., Katayama, T., 2009. Experimental study on ethanol/bentonite slurry injection into synthetic rock fractures: application to seepage control. *Appl. Clay Sci.* 45, 232–238.
- Cheng, D.C.H., 1986. Yield stress: a time-dependent property and how to measure it. *Rheol. Acta* 25, 542–554.
- Chuaqui, M., Bruce, D.A., 2003. Mix design and quality control procedures for high mobility cement based grouts. *Geotech. SP.* 2, 1153–1168.
- Clarke, J.P., 2008. Investigation of Time-dependent Rheological Behavior of Sodium Pyrophosphate-Bentonite Suspensions. Thesis. Purdue University, West Lafayette, IN.
- Coussot, P., 2005. *Rheometry of Pastes, Suspensions and Granular Materials: Applications in Industry and Environment*. Wiley, New York.
- De Paoli, B., Bosco, B., Granta, R., Bruce, D.A., 1992a. Fundamental observations on cement based grouts: traditional materials. In: *Proc. Grouting, Soil Improvement and Geosynthetics, GSP No. 40, ASCE, New Orleans*, pp. 474–495.
- Dzuy, N., Boger, D., 1983. Yield stress measurement for concentrated suspensions. *J. Rheol.* 27, 321–350.
- El Mohtar, C.S., Clarke, J.P., Bobet, A., Santagata, M., Drnevich, V., Johnston, C., 2008. Cyclic response of a sand with thixotropic pore fluid. In: *Proc. Geotech Earthquake Soil Dyn Congr., Sacramento, CA*, pp. 1–10.
- Haldavnekar, V., Bobet, A., Santagata, M., and Drnevich, V. (2003). Soil Treatment with a Thixotropic Fluid: An Autoadaptive Design for Liquefaction Prevention. ICSDEE and Committee TC-4 of ISSMGE, Proceedings of the 11th International Conference on Soil Dynamics & Earthquake Engineering and 3rd International Conference on Earthquake Geotechnical Engineering. Berkeley, CA. Vol. 2, pp. 553–560.
- Hwang, H., 2010. The Effects of Prehydration on Hydraulic Conductivity of SBMs. Thesis. The University of Texas at Austin, Austin, TX.
- Hwang, H., Yoon, J., Rugg, D.A., El Mohtar, C.S., 2011. Hydraulic conductivity of bentonite grouted sand. In: *Proc. the Geofrontiers, Dallas, TX*, pp. 1372–1381.
- Incecik, M., Ceran, I., 1995. Cement grouting model tests. *Bull. Istanbul Tech. Univer.* Istanbul 48, 305–317.
- Karol, R.H., 2003. *Chemical Grouting and Soil Stabilization*, third ed. Marcel Dekker, New York.
- Keentok, M., 1982. The measurement of the yield stress of liquids. *Rheol. Acta* 21, 325–332.
- Kelessidis, V.C., Tsamantaki, C., Dalamarinis, P., 2007. Effect of pH and electrolyte on the rheology of aqueous Wyoming bentonite dispersions. *Appl. Clay Sci.* 38 (1–2), 86–96.
- Kim, Y.S., Whittle, A.J., 2009. Particle network model for simulating the filtration of the microfine cement grout in sand. *J. Geotech. Geoenviron. Eng.* 135, 224–236.

- Luckham, P.F., Rossi, S., 1999. The colloidal and rheological properties of bentonite suspensions. *Adv. Colloid Interface Sci.* 82, 43–92.
- Mahaut, F., Chateau, X., Coussot, P., Ovarlez, G., 2008. Yield stress and elastic modulus of suspensions of noncolloidal particles in yield stress fluids. *J. Rheol.* 52, 287–314.
- Markou, I.N., Atmatzidis, D.K., 2002. Properties and performance of a pulverized fly ash grout. *J. Geotech. Geoenviron. Eng.* 128, 682–691.
- Mitchell, J.K., 1993. *Fundamentals of Soil Behavior*, second ed. Wiley, New York.
- Mittag, J., Salvidis, S.A., 2003. The groutability of sands—results from one-dimensional and spherical tests. In: *Proc. of the 3rd Int. Specialty Conf. on Grouting and Ground Treatment*, ASCE, pp. 1372–1382.
- Moore, D.E., Morrow, C.A., Byerlee, J.D., 1982. Use of swelling clays to reduce permeability and its potential application to nuclear waste repository sealing. *Geophys. Res. Lett.* 9, 1009–1012.
- Ozgulreli, H.G., Vipulanandan, C., 2005. Effect of grain size and distribution on permeability and mechanical behavior of acrylamide grouted sand. *J. Geotech. Geoenviron. Eng.* 131, 1457–1465.
- Penner, D., Lagaly, G., 2001. Influence of anions on the rheological properties of clay mineral dispersions. *Appl. Clay Sci.* 19, 131–142.
- Perret, S., Khayata, K.H., Ballivy, G., 2000. The effect of degree of saturation of sand on groutability—experimental simulation. *Proc. ICE Ground Improv.* 4, 13–22.
- Rugg, D.A., 2010. *Undrained, Monotonic Shear Strength of Loose, Saturated Sand Treated with a Thixotropic Bentonite Suspension for Soil Improvement*, Thesis. The University of Texas at Austin, Austin, TX.
- Rugg, D.A., Yoon, J., Hwang, H., El Mohtar, C.S., 2011. Undrained shearing properties of sand permeated with a bentonite suspension for static liquefaction mitigation. In: *Proc. the Geofrontiers*, Dallas, TX, pp. 677–686.
- Saak, A.W., Jennings, H.M., Shah, S.P., 2001. New methodology for designing self-compacting concrete. *ACI Mater. J.* 98, 429–439.
- Santagata, M.C., Santagata, E., 2003. Experimental investigation of factors affecting the injectability of microcement grouts. In: *Proc. of the 3rd Int. Specialty Conf. on Grouting and Ground Treatment*, ASCE, pp. 1221–1234.
- Santamarina, J., Klein, K.A., Wang, Y.H., Prencke, E., 2002. Specific surface: determination and relevance. *Can. Geotech. J.* 39, 233–241.
- Smoak, G.W., Mitchell, K.D., 1993. Effect of high-range, water-reducers on cement grout. *Concr. Int.* 15, 56–61.
- Stokes, J.R., Telford, J.H., 2004. Measuring the yield behaviour of structured fluids. *J. Non-Newtonian Fluid Mech.* 124, 137–146.
- Tchilingarian, G., 1952. Study of the dispersing agents. *J. Sediment Petrol.* 22, 229–233.
- Zhu, L., Sun, N., Paadopoulos, K., de Kee, D., 2001. A slotted plate device for measuring static yield stress. *J. Rheol.* 45, 1105–1123.